Diode-pumped ultrafast Yb:KGW laser with 56 fs pulses and multi-100 kW peak power based on SESAM and Kerr-lens mode locking

R. AKBARI[1], K.A. FEDOROVA[2], E.U. RAFAILOV[2], A. MAJOR[1]

[1]Department of Electrical and Computer Engineering, University of Manitoba, Winnipeg, R3T 5V6, Canada
[2]Optoelectronics and Biomedical Photonics Group, School of Engineering & Applied Science, Aston University, Birmingham, B4 7ET, UK
Corresponding author: a.major@umanitoba.ca

Abstract A high power sub-60 fs mode-locked diode-pumped Yb:KGW laser based on hybrid action of an InGaAs quantum-dot saturable absorber mirror and Kerr-lens mode locking was demonstrated. The laser delivered a 56 fs pulse with 1.95 W of average power corresponding 450 kW of peak power. The width of the generated laser spectrum was 20.5 nm, which was near the gain bandwidth limit of the Yb:KGW crystal. To the best of our knowledge, these are the shortest pulses generated from the monoclinic double tungstate crystals (and Yb:KGW laser crystal in particular) and the most powerful in the sub-60 fs regime. At the same time, they are also the shortest pulses produced to date with the help of a quantum-dot-based saturable absorber. High power operation with a pulse duration of 90 fs and 2.85 W of average output power was also demonstrated.

1 Introduction

High power operation of ultrashort pulse laser sources is highly desirable for a variety of nonlinear optical experiments [1–4]. The Yb-ion based laser oscillators are well suited for this task. The generation of watt-level sub-100 femtosecond laser pulses directly from Yb-doped bulk crystal lasers has been reported for Yb:KGW [5–7], Yb:CALGO [8,9], Yb:CaF_2 [10–12] and Yb^{3+}:Lu_2O_3 [13] gain media. Such a performance of a mode-locked laser is feasible owing to the propitious properties of Yb-ion crystals, including a fairly broad gain bandwidth, absorption properties suitable for a diode pumping, an absence of parasitic losses and a tolerable level of thermo-optical effects [14–16]. Among the commercially available Yb-doped crystals, Yb:KGW exhibits favorable properties for a high power sub-100 fs pulsed laser: fairly broad amplification bandwidth (~25 nm), high emission cross-section (~2.8 × 10^{-20} cm^2 for E//N_m polarization), and relatively high thermal conductivity (~3.3 W/m/K) [16]. The generation of high power ultrashort pulses with a spectrum as broad as the emission bandwidth of the gain medium is still a demanding task. In the high power regime, the induced nonlinear effects, non-negligible thermal lensing and broad-band group velocity dispersion (GVD) compensation should be carefully addressed. Recently, the generation of 59 fs pulses with 20.2 nm-wide spectrum and output power of 62 mW has been reported from a diode-pumped Kerr-lens mode-locked Yb:KGW laser [17].

The conventional design of a mode-locked laser system based on semiconductor saturable absorber mirrors (SESAMs) offers a flexible procedure and provides a reliable and efficient femtosecond laser performance. However, this method is limited in further shortening of the pulse duration owing to the finite recovery time of an absorber which is also susceptible to damage. On the other hand, the Kerr-lens mode locking technique (KLM) enables one to generate shorter pulses due to its inherently fast saturable absorption-like effect, but it requires careful design procedure and does not usually offer self-starting oscillation [18]. A combination of these two techniques (termed KLAS: Kerr-lens and saturable absorber) can provide a mechanism that benefits from the self-starting operation provided by SESAM as well as the fast loss modulation and broadband operation of the KLM lasers [5,6]. Recently, we reported on the development of a high power sub-100 femtosecond

KLAS mode-locked laser based on an InGaAs quantum-dot SESAM (QD-SESAM) [7] as an alternative approach to the widely used quantum-well SESAMs [5,6]. Such QD-SESAMs exhibit sub-picosecond recovery time, low saturation fluence (10-25 μJ/cm^2), and broad-bandwidth operation. These properties make QD-SESAMs promising candidates for the generation of ultrashort laser pulses [19–21].

In this work, we report on the generation of high power 56 fs pulses from a diode-pumped Yb:KGW laser oscillator based on KLAS mode locking that used a quantum-dot saturable absorber. Using an InGaAs QD-SESAM with a 0.5% modulation depth, the laser delivered 56 fs pulses with 1.95 W of average output power at a repetition rate of 77.3 MHz. This corresponds to ~450 kW of peak power. To the best of our knowledge, these are the shortest pulses generated from the Yb:KGW laser crystal and the shortest ones to date supported by the QD-SESAM structures. Longer pulses with duration of 90 fs and 2.85 W of average power were also generated using high output coupling.

2 Experimental setup

The laser oscillator used a 6 mm-long 1.6 at. % doped Yb:KGW crystal (cut along the N_g-axis) with antireflection (AR) coatings in a Z-fold cavity (Fig. 1). A fiber-coupled diode laser (100 μm, 0.22 NA) delivered maximum power of 30 W at 980 nm. The pump beam was focused to a spot size of 340 μm in the crystal by using two AR-coated achromatic doublets. The absorbed pump power was measured to be around 60%. The laser mode inside the crystal was estimated to be 290 μm in diameter using the ABCD analysis, and it could be gradually increased by adjusting the position of the output coupler mounted on a translation stage. This allowed to introduce the Kerr-lens soft aperturing effect in the mode-locked laser regime owing to a mode size variation with respect to a pump beam waist and a high nonlinear refractive index of the crystal [22]. In the continuous-wave (CW) regime, the laser could deliver up to 6 W of output power using a HR mirror as one of the end mirrors. The laser was polarized along the Nm-axis of the crystal. The thermal lensing of the crystal for the operating range of pump power was estimated to be around 100-150 mm of an equivalent focal length [23]. The QD-SESAM (Innolume GmbH) was grown with 5 pairs of InGaAs quantum dot layers in the saturable structure and had a 0.5% modulation depth with a saturation fluence of 25 μJ/cm^2 [24]. Two Gires-Tournois interferometer mirrors (GTI) were used for compensation of the positive GVD of the laser crystal and optical components, as well as the pulse chirp induced by a self-phase modulation (SPM). The total negative GVD of −3200 fs^2 per round trip was achieved by two bounces on a −550 fs^2 and −250 fs^2 GTI mirrors (Layertec GmbH). The rest of the cavity mirrors were designed to exhibit low GVD at the laser wavelength (Laseroptik GmbH).

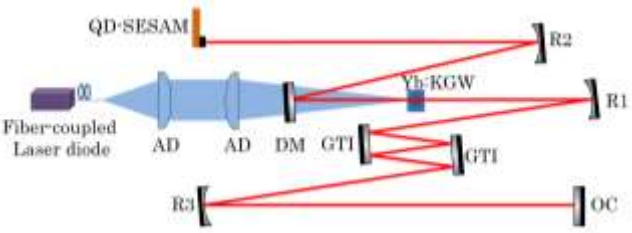

Figure 1. Experimental setup of the mode-locked Yb:KGW laser. AD: achromatic doublets; DM: dichroic mirror; R1-3: concave mirrors; OC: output coupler. R1=300 mm, R2=300 mm and R3=500 mm.

3 Results and discussion

The mode-locked laser operation was initiated by using the QD-SESAM as the end mirror. A stable mode-locked laser with spectral bandwidth of 5-8 nm could be realized. The spectral bandwidth of the pulse depended on the pump power and the separation of the output coupler (OC) and the concave mirror R3 (Fig. 1). The output power was maximized for this regime, and the saturation fluence on the absorber was as high as 270 μJ/cm^2. The Kerr-lensing effect was then introduced by decreasing the OC-R3 distance using a translation stage. This corresponded to the increase of the laser mode size with respect to the pump beam in the crystal. During this procedure the laser underwent multi-pulse oscillation, and the number of pulses per cavity round trip was reduced as the Kerr-lensing effect became more pronounced. A careful adjustment of the pump power was needed during this transition regime. Once the Kerr-lensing effect became sufficiently strong, a stable single-pulse mode-locked laser operation was obtained. With the incident pump power of 18.3 W the laser delivered 56 fs pulses with an average output power of 1.95 W at the repetition rate of 77.3 MHz. The full width at half maximum (FWHM) spectral bandwidth of the laser was measured to be 20.5 nm with a central wavelength of 1040 nm as

shown in Figure 2. The time-bandwidth product (TBWP) was 0.335. At this point, the fluence on the saturable absorber was 370 μJ/cm^2. The single pulse oscillation per round trip was confirmed by using a fast oscilloscope/ photodetector with a temporal resolution of 100 ps in combination with a wide-range scan (200 ps) autocorrelation [25]. Increasing the pump power resulted in multi-pulse oscillation and cessation of the laser oscillation. The radio frequency (RF) spectrum of the pulse train exhibited high signal-to-noise ratio and the absence of Q-switched mode locking instabilities (Fig. 2c).

The spectrum of the generated pulse was accompanied by a narrow spectral component at 1081 nm, which corresponded to the existence of a dispersive wave (Fig. 2b). This dispersive wave, however, was not observed in measurements performed by the oscilloscope and autocorrelator owing to its low intensity and correspondingly long duration. Indeed, the dispersive wave in normal dispersion regime is broadened due to the interplay of SPM and positive GVD at its oscillation wavelength. The net-GVD was calculated based on the available dispersion measurement data of the GTI mirrors, optical components and the Sellmeier coefficients of an undoped KGW crystal [26]. The calculated positive GVD at the dispersive wave oscillation wavelength (1080 nm) was around +4500 fs^2. As it can be seen in Fig. 2b, the total GVD of the cavity rapidly shifted to the normal regime mainly due to the dispersion profile of the −550 fs^2 GTI mirror. The spectral energy of the dispersive wave was estimated to be 6.9% of the total spectral energy, and its presence did not deteriorate the long-term stability of the mode-locked laser. The co-existence of dispersive waves with the main mode-locked pulse has been reported and analyzed previously [27–32]. These waves co-propagate with the main pulse, and some of the pulse energy is coupled out to the dispersive waves if they are phase-matched. The higher order dispersion coefficients have the substantial effect in this regime. A general phase-matching condition can be expressed as [31]

$$D(\omega_n) = \sum_{m\geq 2}\left(\frac{\beta_m}{m!}(-1)^m\omega_n^m\right) + \frac{\beta_2}{2T^2} = \pm 2\pi j, \quad j = 0,1,2,\ldots \quad \textbf{(1)}$$

where $\beta_m = \left.\frac{\partial^m\phi(\omega)}{\partial\omega^m}\right|_{\omega_c}$ are dispersion coefficients, ω_0 is the carrier frequency, $\phi(\omega)$ is the phase delay per round-trip, ω_n is the dispersive wave frequency and $T = \tau/1.76$ where τ is the FWHM of the mode-locked pulse duration.

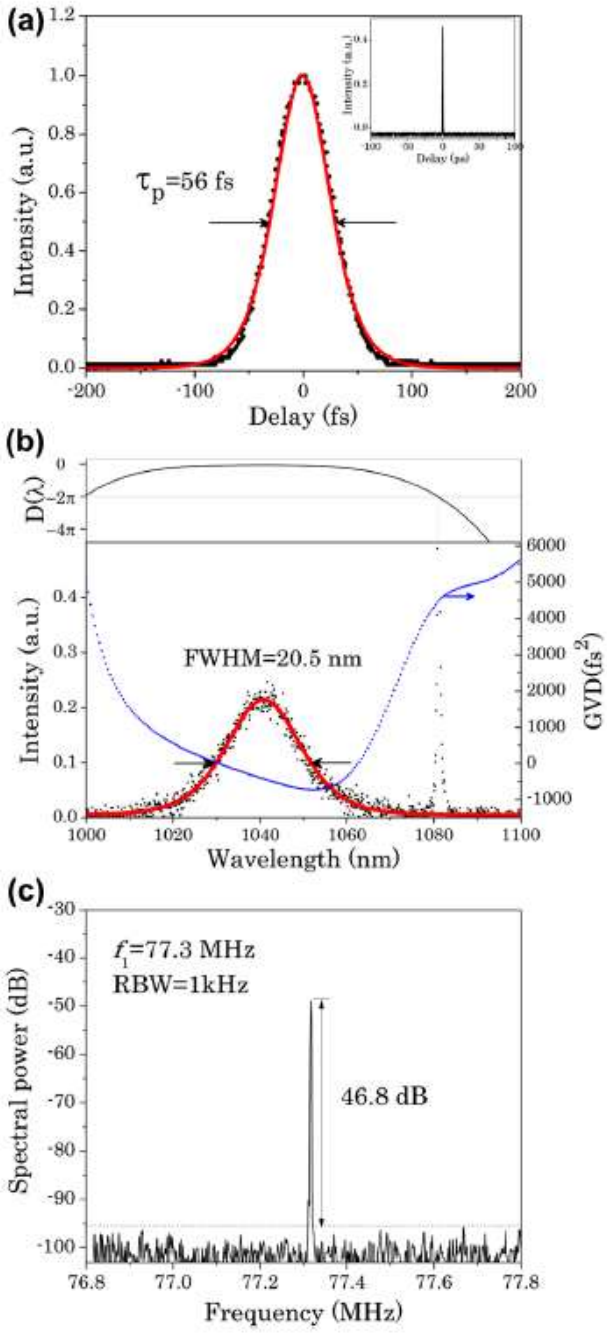

Figure 2. (a) The intensity autocorrelation of the mode-locked laser. Inset: the wide-range scan (200 ps). (b) The spectrum of the mode-locked laser (black dotted curve), the calculated round-trip GVD (blue dotted curve) and the dispersive function $D(\lambda)$ (upper graph). (c) RF spectrum of the pulse train. The sech2-shape fits are shown as red solid curves. RBW resolution bandwidth.

The dispersion coefficients at carrier frequency (1041 nm) were calculated to be β_2=−430 fs^2, β_3=−21451 fs^3, β_4=−4.84×10^6 fs^4 using the net-GVD data. For the measured pulse width of τ=56 fs, the dispersive function D (Eq.1) is plotted in Figure 2(b) (upper curve). The resonance condition was satisfied at the wavelength where the observed dispersive wave was present, i.e. $D(\lambda = 1081\,nm) = -2\pi$. Other possible resonance wavelengths at longer or shorter wavelengths in normal GVD regime were not supported by the effective gain of the laser crystal in combination with the increasing loss of the output coupler and dichroic mirror at those wavelengths. In order to eliminate the dispersive wave, flatter and broader anomalous GVD profile per round-trip for the intended wavelength range is required.

The performance of the laser was also investigated for different GVD and output coupler values (Table 1). The pump power had to be adjusted because of different amount of loss incurred by different number of bounces on combinations of GTI mirrors. By increasing the total negative GVD, longer pulses were generated as expected [5]. The dispersive wave was not observed in case of net-GVD of −4800 fs^2 mainly due to the narrower spectrum of the laser around 1040 nm. With this value of GVD, higher output power could be extracted from the laser cavity by using higher output coupling without significantly compromising the pulse width. For example, 90 fs pulses with 2.85 W of average output power were generated by using 10% output coupling and −4800 fs^2 GVD.

Compared to our previous results of a KLAS mode-locked Yb:KGW laser with a QD-SESAM [7], the generated pulse width was significantly reduced from 90 fs (FWHM=12.5 nm) to 56 fs (FWHM=20.5 nm) by decreasing the net-GVD from −4400 fs^2 to −3200 fs^2, respectively. Our results also showed an enhancement in terms of a pulse duration compared to the previously reported KLAS mode-locked Yb:KGW laser based on a QW-SESAM, where 67 fs pulses with 3 W of output power were generated [6]. We believe that this can be explained by the increased level of SPM due to a longer crystal as well as lower output coupling. The Q-switching instability was also absent during the mode locking procedure, which was attributed to the lower saturation fluence of QD-SESAM. Interestingly enough, the generated 56 fs pulses are also the shortest produced to date with QD-SESAM absorbers (previously, 86 fs pulses were generated from Cr:forsterite laser [19]).

Table 1. Summary of the mode-locked Yb:KGW laser performance.

GTI-GVD* (fs^2)	Output coupler (%)	Pulse width (fs)	Average output power (W)	Dispersive wave	Pump power** (W)
−3200	5	56	1.95	Yes	18.3
−3700	5	68	1.35	Yes	17.5
−4800	5	95	2	No	18.7
−4800	7.5	88	2.5	No	18.6
−4800	10	90	2.85	No	18.9

*The roundtrip net-GVD of GTI mirrors
**The incident pump power

Higher power regime, however, would require careful compensation of a strong thermal lensing effect in Yb:KGW. A promising candidate for this regime is Yb:CALGO crystal with a thermal conductivity coefficient of 6.9 W/m/K and emission bandwidth of 80 nm [33]. For example, the generation of 94 fs pulses with 12.5 W of average output power with SESAM mode locking was reported in [8]. Shorter pulses with a duration of 40 fs at lower output power of 1.1 W was also demonstrated in this crystal by Kerr-lens mode locking technique [9]. Another promising Yb-doped laser crystal for generating high power sub-100 fs pulses is Yb:CaF_2 crystal with a thermal conductivity coefficient of 6 W/m/K and emission bandwidth of 30 nm [34,35]. The generation of 68 fs and 48 fs pulses with output powers of 2.3 W and 2.7 W using the Kerr-lens mode locking have been reported in [12] and [10], respectively. It should be noted that results presented in [9,10] and [12] were not obtained with directly diode-pumped lasers which greatly reduces their overall efficiency and potential for further power scaling. Therefore, the use of commercially available laser diodes for direct diode pumping is a desired feature due to the reduced cost and complexity of the laser system. A diode-pumped SESAM mode-locked Yb:CaF_2 laser was also demonstrated, delivering 87 fs pulses with 1.4 W of output power [11]. A new laser crystal, Yb^{3+}:Lu_2O_3, with thermal conductivity of 11 W/m/K and emission bandwidth of 13 nm has also shown its potential in this regime [36]. The generation of 71 fs pulses with 1.09 W of average power was reported in [13]. A comparison of performance of the diode-pumped Yb-lasers in the sub-100 fs regime is shown in Figure 3. As can be seen, the generated 56 fs pulses with 450 kW of peak power in our work demonstrate more than one order of magnitude higher average and peak powers when compared

to the previous sub-60 fs diode-pumped Yb-lasers [37–42]. We believe that such a powerful ultrashort pulse laser source will be attractive for nonlinear frequency conversion into the visible and near-infrared ranges [43–45].

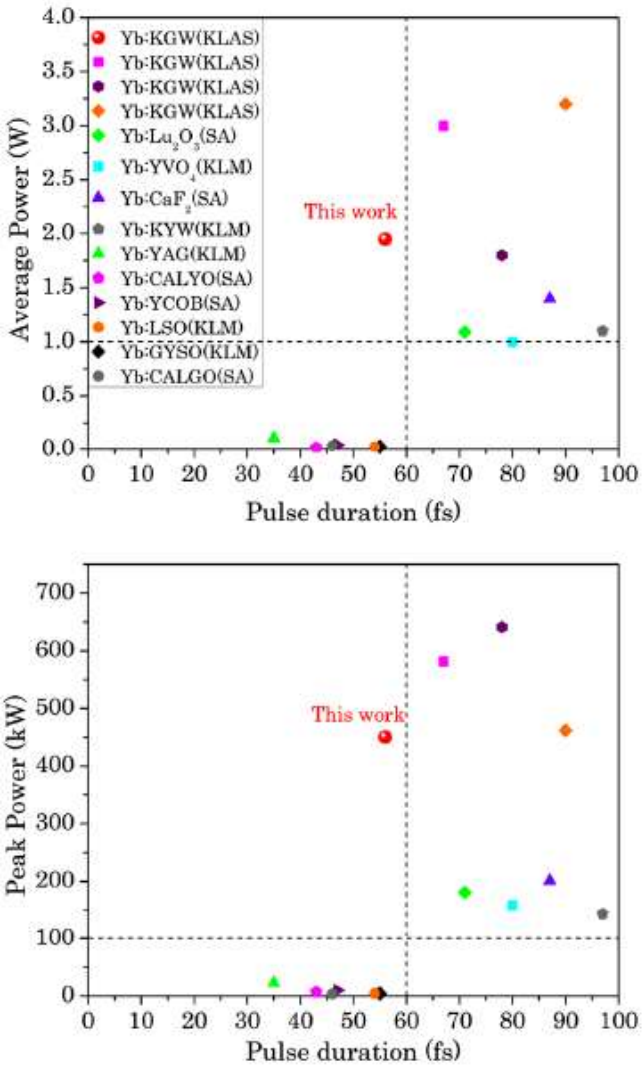

Figure 3: Comparison of sub-100 fs diode-pumped Yb-doped crystal lasers [5–7, 11, 13, 37-42, 46]. Data from Ref. [8] are not shown for scaling reasons to better visualize the <90 fs regime. SA: saturable absorber, SESAM.

4 Conclusion

In summary, a high power sub-60 fs Yb:KGW laser mode-locked using KLAS mode locking with a QD-SESAM was demonstrated. The laser delivered 56 fs pulses with 1.95 W of average power, which is, to the best of our knowledge, the shortest pulse duration generated from the monoclinic double tungstate crystals and the Yb:KGW crystal in particular. The output average and peak powers were an order of magnitude higher than previously reported values. The QD-SESAM was used to initiate and sustain the pulse generation while the Kerr-lens mode locking effect was introduced for the further pulse duration shortening and stabilization of the single-pulse regime. The spectral bandwidth of the mode-locked laser was 20.5 nm which was near the emission bandwidth limit of the Yb:KGW laser crystal (~25 nm). The pulse duration was limited by the appearance of the dispersive wave at longer wavelength which was caused by the increased level of uncompensated dispersion. This fact and the underutilized emission bandwidth point out to the possibility of generation of even shorter pulses. This can be achieved by more careful dispersion management. At the same time, using a more broadband emission with the Ng-polarisation of Yb:KGW [47] or gain media such as Yb:CALGO will be also beneficial. Our preliminary KLAS mode locking results with this crystal indicate that the generation of powerful sub-50 fs pulses is possible [48] and will be the subject of future publication. The use of a lower output coupling to reduce the gain [49] can be another route to shorter pulses albeit at the price of a lower output power.

Funding. Natural Sciences and Engineering Research Council of Canada (NSERC); University of Manitoba; Western Economic Diversification Canada (WD).

References

1. A. Major, D. Sandkuijl, and V. Barzda, Opt. Express **17**, 12039 (2009).
2. D. Sandkuijl, R. Cisek, A. Major, and V. Barzda, Biomed. Opt. Express **1**, 895 (2010).
3. R. Akbari and A. Major, Laser Phys. **23**, 35401 (2013).
4. A. Major, F. Yoshino, J. S. Aitchison, P. W. E. Smith, E. Sorokin, and I. T. Sorokina, Appl. Phys. Lett. **85**, 4606 (2004).
5. H. Zhao and A. Major, Opt. Express **22**, 30425 (2014).
6. H. Zhao and A. Major, Opt. Express **21**, 31846 (2013).
7. R. Akbari, H. Zhao, K. A. Fedorova, E. U. Rafailov, and A. Major, Opt. Lett. **41**, 3771 (2016).
8. A. Greborio, A. Guandalini, and J. Aus der Au, Proc. SPIE **8235**, 823511 (2012).
9. P. Sevillano, P. Georges, F. Druon, D. Descamps, and E. Cormier, Opt. Lett. **39**, 6001 (2014).
10. P. Sevillano, G. Machinet, R. Dubrasquet, P. Camy, J.-L. Doualan, R. Moncorge, P. Georges, F. P. Druon, D. Descamps, and E. Cormier, in Advanced Solid-State Lasers Congress (OSA, 2013), p. AF3A.6.
11. F. Pirzio, S. D. Di Dio Cafiso, M. Kemnitzer, F. Kienle, A. Guandalini, J. Aus der Au, and A. Agnesi, J. Opt. Soc. Am. B **32**, 2321 (2015).

12. G. Machinet, P. Sevillano, F. Guichard, R. Dubrasquet, P. Camy, J.-L. Doualan, R. Moncorgé, P. Georges, F. Druon, D. Descamps, and E. Cormier, Opt. Lett. **38**, 4008 (2013).
13. M. Tokurakawa, A. Shirakawa, K. Ueda, R. Peters, S. T. Fredrich-Thornton, K. Petermann, and G. Huber, Opt. Express **19**, 2904 (2011).
14. W. F. Krupke, IEEE J. Sel. Top. Quantum Electron. **6**, 1287 (2000).
15. P. A. Loiko, K. V. Yumashev, N. V. Kuleshov, and A. A. Pavlyuk, Appl. Phys. B **106**, 663 (2012).
16. S. R. Bowman, S. P. O'Connor, and S. Biswal, IEEE J. Quantum Electron. **41**, 1510 (2005).
17. M. Kowalczyk, J. Sotor, and K. M. Abramski, Laser Phys. Lett. **13**, 35801 (2016).
18. U. Keller, Appl. Phys. B **100**, 15 (2010).
19. A. A. Lagatsky, C. G. Leburn, C. T. A. Brown, W. Sibbett, S. A. Zolotovskaya, and E. U. Rafailov, Prog. Quantum Electron. **34**, 1 (2010).
20. E. U. Rafailov, M. A. Cataluna, and W. Sibbett, Nat. Photonics **1**, 395 (2007).
21. E. U. Rafailov, S. J. White, A. A. Lagatsky, A. Miller, W. Sibbett, D. A. Livshits, A. E. Zhukov, and V. M. Ustinov, IEEE Photonics Technol. Lett. **16**, 2439 (2004).
22. A. Major, J. S. Aitchison, P. W. E. Smith, F. Druon, P. Georges, B. Viana, and G. P. Aka, Appl. Phys. B **80**, 199 (2005).
23. H. Mirzaeian, S. Manjooran, and A. Major, Proc. SPIE **9288**, 928802 (2014).
24. A. A. Lagatsky, F. M. Bain, C. T. A. Brown, W. Sibbett, D. a. Livshits, G. Erbert, and E. U. Rafailov, Appl. Phys. Lett. **91**, 231111 (2007).
25. T. Waritanant and A. Major, Opt. Express **24**, 12851 (2016).
26. M. C. Pujol, M. Rico, C. Zaldo, R. Solé, V. Nikolov, X. Solans, M. Aguiló, and F. Díaz, Appl. Phys. B **68**, 187 (1999).
27. M. J. P. Dymott and A. I. Ferguson, Appl. Phys. B **65**, 227 (1997).
28. F. Salin, P. Grangier, P. Georges, and A. Brun, Opt. Lett. **15**, 1374 (1990).
29. S. Ozharar, I. Baylam, M. N. Cizmeciyan, O. Balci, E. Pince, C. Kocabas, and A. Sennaroglu, J. Opt. Soc. Am. B **30**, 1270 (2013).
30. V. L. Kalashnikov, E. Sorokin, and I. T. Sorokina, J. Opt. Soc. Am. B **18**, 1732 (2001).
31. Q. Lin and I. Sorokina, Opt. Commun. **153**, 285 (1998).
32. P. F. Curley, C. Spielmann, T. Brabec, F. Krausz, E. Wintner, and A. J. Schmidt, Opt. Lett. **18**, 54 (1993).
33. J. Petit, P. Goldner, and B. Viana, Opt. Lett. **30**, 1345 (2005).
34. M. Siebold, S. Bock, U. Schramm, B. Xu, J. L. Doualan, P. Camy, and R. Moncorgé, Appl. Phys. B **97**, 327 (2009).
35. J. Boudeile, J. Didierjean, P. Camy, J. L. Doualan, A. Benayad, V. Ménard, R. Moncorgé, F. Druon, F. Balembois, and P. Georges, Opt. Express **16**, 10098 (2008).
36. U. Griebner, V. Petrov, K. Petermann, and V. Peters, Opt. Express **12**, 3125 (2004).
37. A. Yoshida, A. Schmidt, V. Petrov, C. Fiebig, G. Erbert, J. Liu, H. Zhang, J. Wang, U. Griebner, Opt. Lett. 36, 4425 (2011).
38. A. Agnesi, A. Greborio, F. Pirzio, G. Reali, J. Aus der Au, A. Guandalini, Opt. Express 20, 10077 (2012).
39. F. Pirzio, S.D.D.D. Cafiso, M. Kemnitzer, A. Guandalini, F. Kienle, S. Veronesi, M. Tonelli, J. Aus der Au, A. Agnesi, Opt. Express 23, 9790 (2015).
40. J. Zhu, Z. Gao, W. Tian, J. Wang, Z. Wang, Z. Wei, L. Zheng, L. Su, J. Xu, Appl. Sci. 5, 817 (2015).
41. W.-L. Tian, Z.-H. Wang, J.-F. Zhu, Z.-Y. Wei, L.-H. Zheng, X.-D. Xu, J. Xu, Chin. Phys. Lett. 32, 24206 (2015).
42. S. Uemura, K. Torizuka, Jpn. J. Appl. Phys. 50, 10201 (2011).
43. H. Zhao, I.T. Lima Jr., A. Major, Laser Phys. 20, 1404 (2010).
44. I.T. Lima Jr., V. Kultavewuti, A. Major, Laser Phys. 20, 270 (2010).
45. S. Manjooran, H. Zhao, I.T. Lima Jr., A. Major, Laser Phys. 22, 1325 (2012).
46. F.M. Bain, A.A. Lagatsky, C.T.A. Brown, W. Sibbett, Proc. SPIE 6871, 68712L (2008).
47. A. Major, D. Sandkuijl, V. Barzda, Laser Phys. Lett. 6, 779 (2009).
48. S. Manjooran and A. Major, in Conference on Lasers and Electro-Optics (OSA, 2016), p. JTu5A.82.
49. H. Zhao, A. Major, Opt. Express 22, 26651 (2014).